Circular non-uniform electric field gel electrophoresis for the separation and concentration of nanoparticles

Lu Liu, [a] Ruilin Yang, [b] Jiaxuan Cui, [a] Peng Chen, [b] Hyok Chol Ri, [c] Huaze Sun, [a] Xiangfan Piao, [d] Minshu Li, [e] Qiaosheng Pu, [f] Maurizio Quinto, [g] John L. Zhou, [h] Hai-Bo Shang** [a,b] and Donghao Li* [a,b]

[a] Department of Chemistry, Yanbian University, Park Road 977, Yanji City 133002, Jilin Province, China
[b] Interdisciplinary Program of Biological Functional Molecules, College of Integration Science, Yanbian University, Park Road 977, Yanji City 133002, Jilin Province, China
[c] College of Pharmacy, Yanbian University, Park Road 977, Yanji City 133002, Jilin Province, China
[d] Department of Electronics, School of Engineering, Yanbian University, Park Road 977, Yanji City 133002, Jilin Province, China
[e] Department of pharmacy, University of Copenhagen, Copenhagen, 2100, Denmark.
[f] State Key Laboratory of Applied Organic Chemistry, Key Laboratory of Nonferrous Metals Chemistry and Resources Utilization of Gansu Province, Department of Chemistry, Lanzhou University, Lanzhou, Gansu 730000, China
[g] DAFNE - Department of Agriculture, Food, Natural Resources and Engineering, University of Foggia, Via Napoli 25, I-71122, Foggia, Italy
[h] Centre for Green Technology, School of Civil and Environmental Engineering, University of Technology, Sydney, Ultimo 2007, Australia

Author Contact Information:

*Donghao Li, Ph.D. (corresponding author)

Phone: +86-433-2436456

Fax: +86-433-2432456

E-mail: dhli@ybu.edu.cn

Hai-Bo Shang, Ph.D (co-corresponding author)

Phone: +86-473-2432456

Fax: +86-473-2432456

E-mail: hbshang@ybu.edu.cn

Abstract

A circular non-uniform electric field strategy coupled with gel electrophoresis was proposed to control precise separation and efficient concentration of nano- and micro-particles. The circular non-uniform electric field has the feature of exponential increase in electric field intensity along the radius, working with three functional zones of migration, acceleration, and concentration. Distribution form of electric field lines is regulated in functional zones to control the migration behaviors of particles for separation and concentration by altering the relative position of the ring electrode (outside) and rodlike electrode (inner). The circular non-uniform electric field promotes the target-type and high-precision separation of nanoparticles based on the difference of charge-to-size. The concentration multiple of nanoparticles is also controlled randomly with the alternation of radius, taking advantage of vertical extrusion and concentric converging of the migration path. This work provides brand-new insight about simultaneous separation and concentration of particles and is perspective to develop a versatile tool for separation and preparation of various samples instead of conventional methods.

Key words: non-uniform electric field, target-type, precise separation, concentration

Introduction

Definitely, it's greatly significant to efficiently separate, purify and concentrate micro/nanoscale objects in various fields,[1-4] such as synthesis of micro/nano fabrication with an ultranarrow size distribution, early-stage diagnosis and therapy of diseases, accurate detection of biological samples, and cell screening.[5-8] However, there are still some confronting problems of a complex matrix, low concentration of objects, poor size uniformity, resulting in difficulty of highly purified preparation and sensitive detection, not satisfy the practical requirements.[9,10] So, it's urgent to develop new techniques for precise separation and efficient concentration of micro/nanoscale objects.

Precise separation is the premise to realize quality monitoring in various fields. The conventional batch separation techniques has been developed based on size, density, charge, and marker proteins modified on the surface, respectively, including size exclusion chromatography,[11] field-flow fractionation,[12,13] pinched flow fractionation,[14,15] density gradient centrifugation[16] and immunoaffinity capture.[17] Some sieving separation microfluidic methods as new methods have been developed for separation or isolation of micro/nanoscale objects from the complex matrix, including microfluidic filtration,[18,19] micropillar array,[20,21] nanowire capture technology,[22] and deterministic lateral displacement sorting,[23,24] inertial separation,[25] etc. However, there are several inevitable drawbacks of the complex device, low throughput, tedious procedures, and negative effects on the downstream analysis for practical operations.[10]

For the highly sensitive detection and preparation, some techniques come into sight for efficient concentration. As a typical label method, active-based magnetic bead is to capture the target objects by surface modification,[26,27] not suitable for the following analysis. In contrast,

label-free strategies provide the insight of continuous flow concentration or point-focus. Microfluidic centrifugation[28-30] can compel migration of the desired sample to the outer wall with the following concentration at outlet, and membrane electrophoresis could intercept big size of objects based on size effect for concentration.[6,31] Besides, the acoustic-based platform uses the acoustic wave to sort and concentrate objects.[32-34] Typically, dielectrophoresis is widely used with the functions of trapping and enrichment of cells or particles by employing the non-uniform electric fields.[35-39] Although great efforts in concentration methods, some critical problems still exist to seriously prevent methods promotion, such as less variety of samples, time-consuming, hard to collect, and sample loss. Meanwhile, the unique technique is scarce to achieve simultaneous separation and concentration. Hence, it is of significant to provide a new way of developing the integrative and controlled device for precise separation and efficient concentration.

In view of this, a circular-electric-gradient agarose gel electrophoresis was proposed to simultaneously separate and concentrate objects by one-step, which is spired by the target distribution of the Milky Way. The system is spired by the circle-gradient field and efficient separation of gel electrophoresis like chromatography. The common slab gel electrophoresis is carried out under the uniform electric field driving with drawbacks of lower separation resolution, more importantly, without concentration of objects.[40-43] So the circular gel electrophoresis coupled with non-uniform electric field is put forward to replace traditional type. In this system, the electrodes are set at the center and edge of circular gel, and objects of different sizes distribute as concentric circles for separation in consistent with target-type gradient electric intensity. Not only that, the sample circle could continuously migrate until focused near the center for concentration because of contraction in terms of radius. The characteristics of circular-electric field were

presented by the numerical simulation, and the migration behaviors of objects were also investigated under various parameters, including the gel concentration, electrophoresis voltage and time, type of non-uniform electric field. To verify the technical feasibility, it was applied to separate and concentrate the gold nanoparticles.

Materials and methods

Materials and Reagents. 30 and 60 nm gold nanoparticles were obtained from BBI Life Science Co., Ltd (Shanghai, China). 5.0×TBE buffer (pH 8.0-8.6) was from Sangon Biotech Co., Ltd. (Shanghai, China) and stored at 4℃. Sodium hydroxide (≥98%) was purchased from Macklin Biochemical Co., Ltd (Shanghai, China). Regular AGAROSE G-10 was obtained from Biowest (Beijing, China). The platinum wire (ID=0.22 mm) was purchased from Lucheng Metal Processing Factory (Tianjin, China). Ultrapure water was prepared by the water purifier (Milli-Q Integral, America).

Instruments. A PowerPac Basic electrophoresis instrument was applied to support all electrophoresis experiments (Junyi, JY300C, China). The scanning electron microscope (SEM) images were obtained by a Hitachi Regulus 8100 scanning electron microscopy (Tokyo, Japan), and transmission electron microscopy (TEM) analysis was carried out on a Tecnai G2 F20 field emission transmission electron microscope (FEI, America). A 90Plus Zeta dynamic light scattering (DLS) was used to evaluate the size distribution of nanoparticles (Brookhaven, America). All the electric field simulation data were performed using the COMSOL 5.4 Multiphysics software.

Preparation of special device for gel electrophoresis. The device is mainly composed of power supply system, separation system, collection system, circulation system, and cooling system

(Figure S1a). Among these, the cycloidal agarose gel as separation system (Figure S1b) was fabricated as follows: Generally, a certain amount of agarose was dissolved in 20 mL 1×TBE solution (obtained by diluting 10×storage solution) (pH=8.2) under microwave-assisted heating for 2 min and waiting for cooling at 55℃, after that the solution was immediately poured into the $50 \times 50 \times 12$ mm^3 culture dish, and then the sample loading mould (Figure S1c, d for hole-type sampling, Figure S1e, f for ring-type sampling) was successively fixed into the agarose gel, followed by cooling to room temperature for 30 min. The transparent gel was subsequently transferred to electrophoresis chamber bath containing 1×TBE running buffer after removing the mould. Finally, the platinum wire (positive electrode) and the tin foil ring were placed in the center and edge of circular gel, respectively, as the internal and the external electrodes to build the non-uniform electric field. Particularly, the design of circulation and cooling system can effectively avoid the negative effect of circumstances varying on separation (Figure S2).

Electrophoretic separation of 30 nm and 60 nm gold nanoparticles. The separation of gold nanoparticles was performed as the following procedure. The 30 and 60 nm nanoparticles were dispersed via ultrasound for 10 min before use to avoid the nanoparticles aggregation, the certain volume of mixture including 20 μL glycerol and 400 μL nanoparticles were loaded into the sample loop for investigating the separation under different parameters, such as electrophoresis time and voltage, concentration of agarose.

Results and discussion

As an example, 30 and 60 nm gold nanospheres are chosen to study electric field characteristics and migration behaviors under the circular non-uniform electric field, which are

named “30 nm AuNPs” and “60 nm AuNPs” in the following text. Transmission electron microscopy (TEM) images show most gold nanoparticles as spheres, a small number of particles as triangles, and the particle size is also inhomogeneous with wide distribution, but the percentage of nanoparticles close to 30 nm and 60 nm is highest to 23.3% and 22.8% calculated by TEM (Figure 1a, b). Dynamic light scattering (DLS) results also demonstrate the size distribution from 20-58 nm for 30 nm AuNPs, 40-110 nm for 60 nm AuNPs, because of the nanoparticles aggregation (Figure 1c). 30 nm and 60 nm AuNPs are electronegative with zeta potential of -49.8±3.2 mV (mean±SD) and -30.1±2.1 mV in TBE buffer (pH=8.2), respectively (Figure 1d). 30 nm AuNPs obviously have a higher charge-to-size ratio than 60 nm AuNPs (Figure 1e), indicated that under the circular-electric-gradient agarose gel electrophoresis, the electrophoretic mobility of 30 nm AuNPs is higher than 60 nm AuNPs in the influence of non-uniform electric field effect and the size effect of gel medium, which is expected to achieve efficient and precise separation.

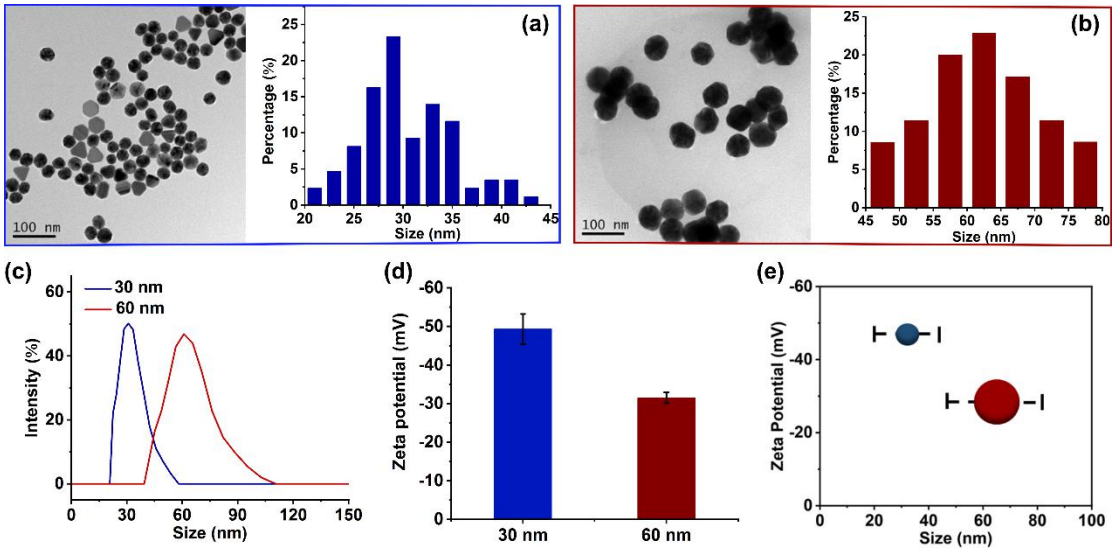

Figure 1. Typical TEM images of AuNPs and size distribution calculated by corresponding TEM data: (a) 30 nm, (b) 60 nm, the total numbers of nanoparticles were analyzed by using the software ImageJ. Each sample showed more than 100 particles to provide a good representativeness of the

separation results. (c) Size distribution measured by DLS, (d) Zeta potential of AuNPs, (d) Comparison of size and zeta potential of 30 nm (blue) and 60 nm (red) AuNPs.

The COMSOL simulation was applied to investigate the characteristics of the circular non-uniform electric field. When the positive electrode (rod-shape) in the center and a negative electrode (ring-shape) around the edge are set in parallel at the same height (Figure 2a), the electric intensity is strongest in the center with divergent reduction of gradient until to the weakest at the edge (defined as non-uniform field-1) (Figure 2b). The equipotential lines present the concentric circles with the density difference along radius, like target (Figure 2c). The integration of electric intensity and equipotential lines is shown in Figure 2d. In addition, the electric intensity is equivalent in the longitudinal section (Figure 2e). The movement of the micro-objects has a certain resistance (f′) under the action of electric field force (F_{ep}) (Figure 2f). In the horizontal direction, the resultant force can be regarded as $F=F_{eq}-f'=qE-f'$, in which f′and q remain unchanged, F is proportional to E. Thus, the same micro-objects could be migrated in accordance with one circle of equipotential lines under the gradient voltage in the concentric electrophoresis device. If the q and f′ are different under the same E, the nanoparticles are separated according to the concentric distribution of equipotential lines based on the difference in charge-to-size. Therefore, under the circular non-uniform electric field in horizontal, the nanoparticles would be driven by the stronger electrophoretic force (F_{ep}) and separated with the target-type distribution on the base of the charge-to-size difference (Figure 2g).

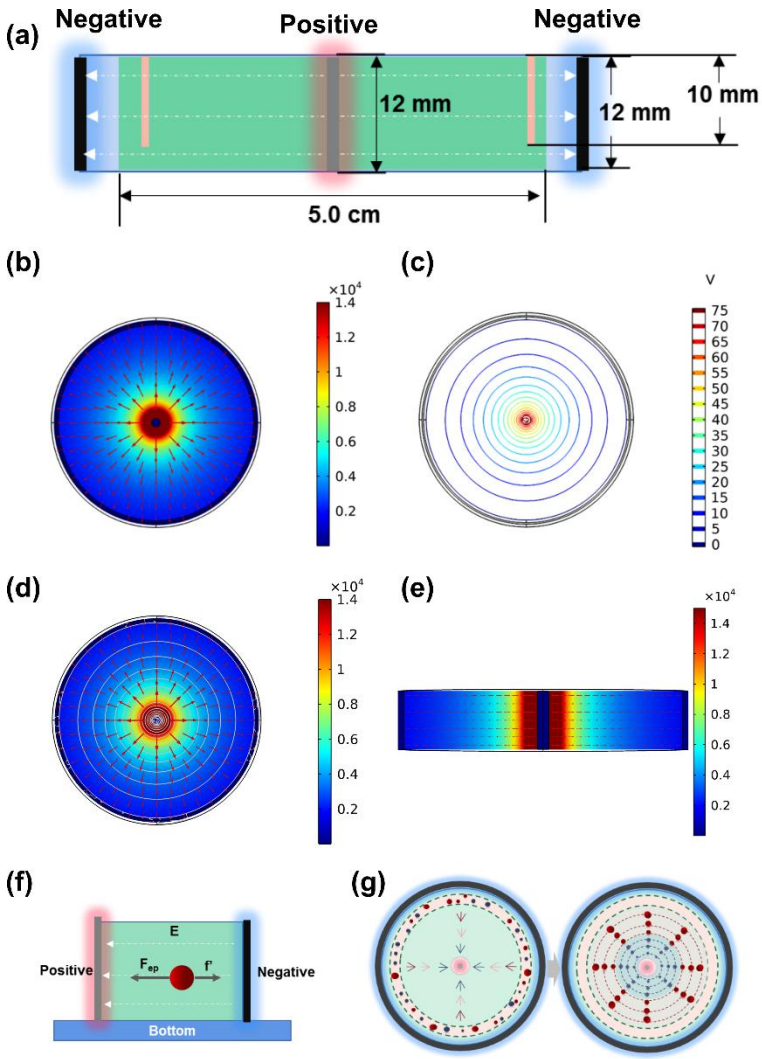

Figure 2. (a) Scheme of relative position of negative and positive electrodes. COMSOL simulation of circular non-uniform field 1. (b) electric field intensity, (c) equipotential lines, (d) integration of electric intensity and equipotential line, (e) cross section, (f) Force analysis of nanoparticle under circular non-uniform field 1 (the voltage was set at 75 V). F_{ep} represents the electrophoretic force and f′ represents the viscous force. (g) Scheme of precise target-type distribution of nanoparticles with size difference under circular non-uniform field 1.

According to the above COMSOL simulation discussed, the circular electrophoresis system provides a non-uniform gradient electric field with circle of equipotential lines, which will greatly

affect separation behavior of the object. Besides, the pore size is also one of the major factors affecting on the migration and separation behavior of objects in the electrophoresis technique. The concentration of agarose gel is related to pore size. The pore size of agarose gel decreases with the increase of gel concentration from 0.8% to 1.2% (Figure 3a). The electrophoretic separation is more significant with the bigger pore size (Figure 3b, 3c). The migration velocities of nanoparticles are slower on the higher concentration agarose gel, due to the overlying of the size exclusion effect. Significantly, the obvious difference of migration distances for 30 and 60 nm AuNPs is presented on the 0.8% agarose gel after 30 min electrophoresis (Figure 3c). Furthermore, it is interested that the migration velocity of AuNPs is greatly increasing close to the center, generating the rapid concentration effect, which is completely consistent with the gradient increase of electric field intensity from edge to center. The above experimental results demonstrate that the low electric field intensity (periphery) and the low concentration agarose gel (large pore size) are favorable for separation, and the high electric field region (center) are advantageous for rapid concentration in circular non-uniform electric field gel electrophoresis system.

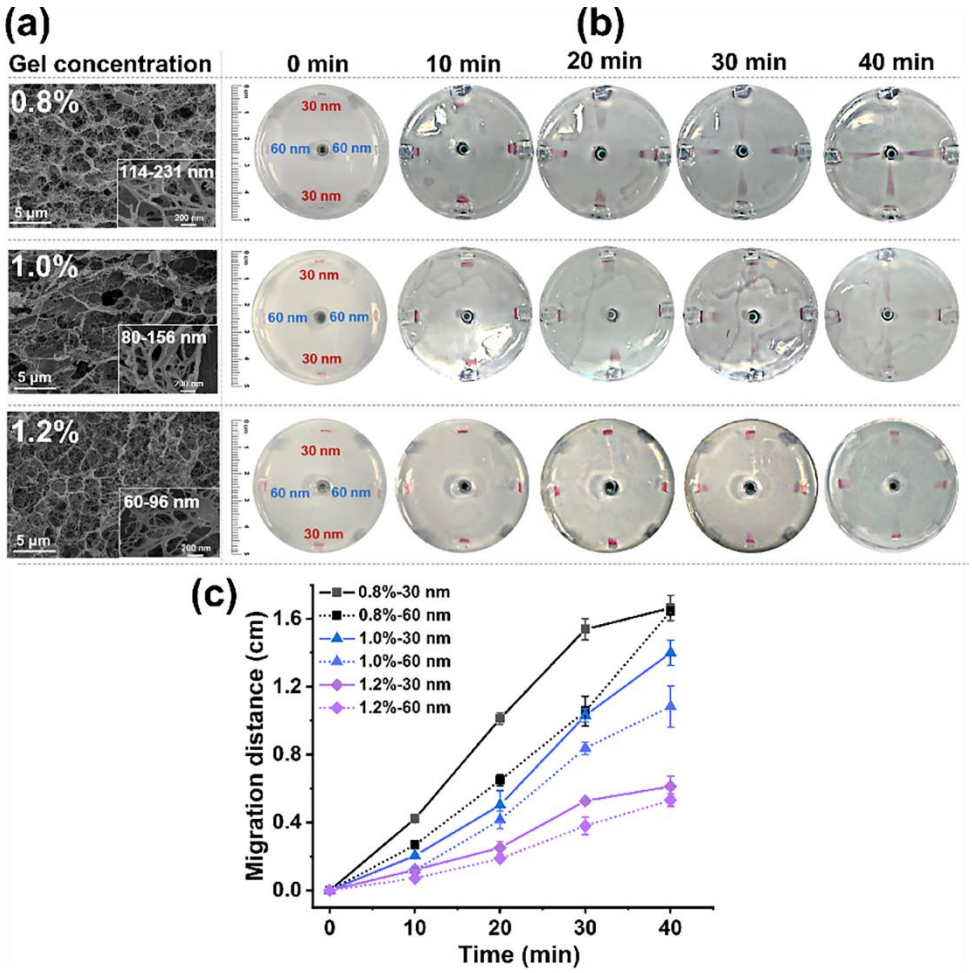

Figure 3. Effect of agarose gel prepared by different concentrations on the migration of 30 and 60 nm AuNPs. The applied voltage was set at 75V, the buffer solution was 1×TBE (pH=8.2). (a) SEM images for pore size of agarose gel, (b) Migration images of AuNPs with electrophoresis time on the circular agarose gel, (c) Comparison of migration distance of AuNPs with electrophoresis time.

Based on the above experimental results, we focus on the relationship between electric field density and particle migration behavior under annular electric field. According to the curve of electric field intensity and radius from COMSOL simulation, the electric field intensity increases exponentially with the reduction of radius under the circular non-uniform electric field 1 (Figure

4a). The whole non-uniform electric field could be divided into migration zone, acceleration zone, and concentration zone based on the increasing degree in field intensity per unit distance. However, the concentration zone is near to the central electrode cell, so the regulation in the migration zone and acceleration zone determines the separation of nanoparticles. As expected, the electric field distribution of migration zone and acceleration zone is positive correlation with electric voltage (Figure 4b). Under the same voltage, the electrophoretic velocity of 30 nm AuNPs is larger than that of 60 nm AuNPs during the whole electrophoretic process and the gap in migration velocity enlarges progressively as increasing voltage for 30 and 60 nm AuNPs (Figure 4c-e). The bigger voltage makes, the faster the migration velocity and the wider band of nanoparticles close to the central electrode, corresponding to the increase of the electric field gradient with the decrease of radius.

In equilibrium theory of forces, F_{ep} increases with the gradient enhancement of E, promoting the increase of the electrophoretic velocity, in which f˝ and q remain unchanged. It's logical that 30 nm AuNPs with bigger charge-to-size first migrated to the acceleration zone for separation under the same voltage. At 50 V, AuNPs passed through the migration zone with a slower migration velocity, resulting in the poor separation (Figure 4f). At 75 V, nanoparticles could migrate to the acceleration zone in turn (radius $\leq$ 1.25 cm). Because of the strong electric field in the acceleration zone, the 30 nm AuNPs is accelerated and enlarging the gap of migration velocity of AuNPs due to the time difference with different charge-to-size, and further realizing the accurate separation (Figure 4g). Although the bigger voltage is more favorable for the highly accurate separation based on the above analysis, the heating effect could cause deformation of agarose gel under high voltage (Figure 4h), so the voltage of 75 V was chosen for the following

separation.

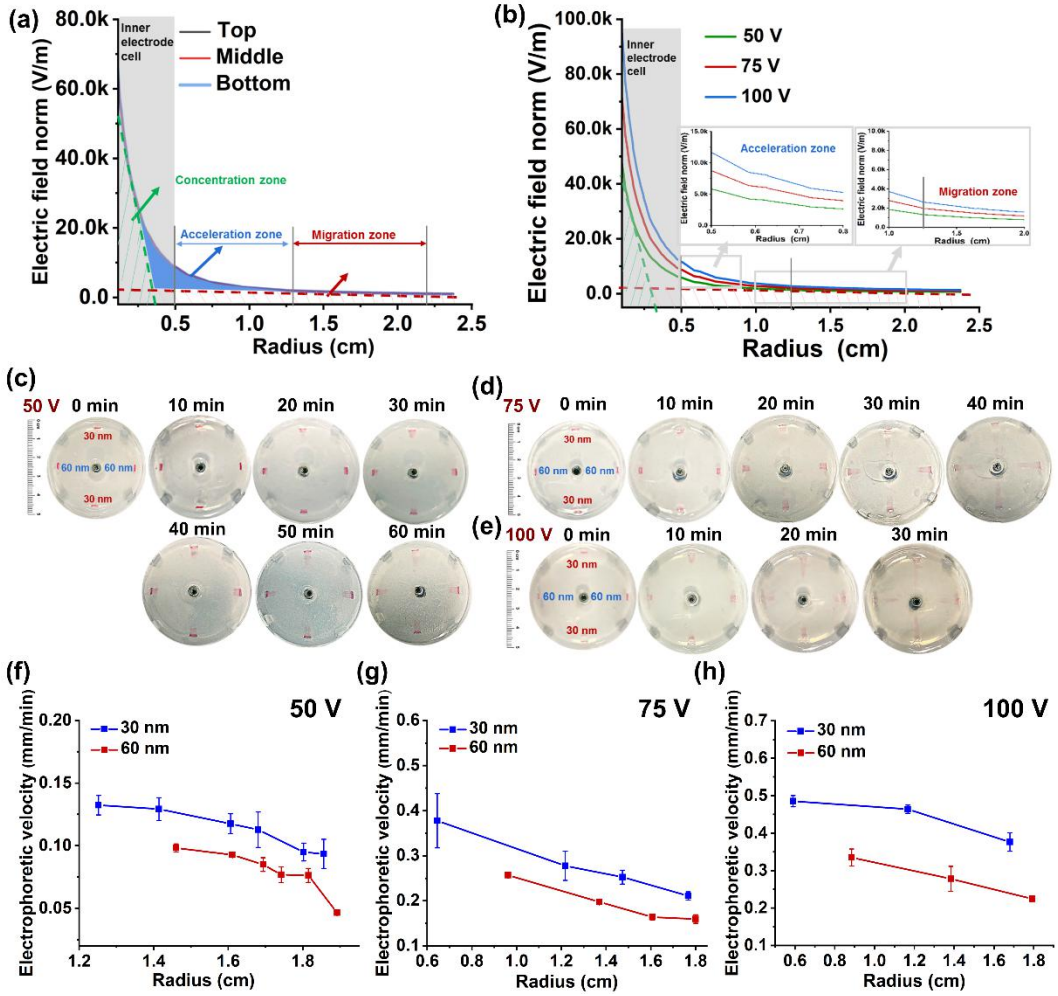

Figure 4. (a) Typical curve of electric field norm and radius from COMSOL simulation for the circular non-uniform electric field 1 in horizontal and longitudinal (75 V). (b) Comparison of curves of electric field norm and radius at different voltages from COMSOL simulation (50 V, 75 V, 100 V). (c-e) Migration images of 30 nm and 60 nm AuNPs with electrophoresis time at different voltages. (f-h) Comparison of the electrophoretic velocity of 30 nm and 60 nm AuNPs at 50, 75 and 100 V voltage, respectively. The experiment was performed under the 0.8% agarose gel and the 1×TBE (pH=8.2) buffer solution.

In order to quantify the separation efficiency, the hole-type sampling method was applied.

The hole-type sampling mentioned above is more conventional to investigate the migration behavior of nanoparticles. The ring-type sampling is visual to present the target-type separation of nanoparticles under the circular non-uniform electric field. The two concentric bands were shaped with the difference of migration velocity for 30 nm and 60 nm AuNPs, and the bands broadened gradually with the extension of electrophoresis time (Figure S3a, b). It is due to the wide size distribution of the so-called standard sample and the sample was further separated subtly based on the tiny size difference in acceleration zones, which is demonstrated by the TEM and size distribution results of different fractions along horizontal lines (Figure S3c-f).

Furthermore, the mixture of 30 and 60 nm AuNPs was applied to verify the feasibility of controlled and precise separation. After electrophoresis for 20 min, the two clear bands with concentric circle type appear in the migration zone, front-end for 30 nm particles and back-end for 60 nm particles (Figure 5a). The TEM results of fractions from every sample band indicate precision separation with normal size distribution (Figure 5b) (The fraction sampling is the same as that shown in (Figure S3)), but the size overlap of 30 nm and 60 nm AuNPs still remains in accordance with the original size distribution of DLS detection (Figure 5c). Obviously, after electrophoresis for 30 min, in acceleration zone, the separation resolution improves with narrower size distribution of every fraction and the blank distribution tape between 30 nm and 60 nm AuNPs (Figure 5d-f). In addition, the AuNPs percentage of different sizes in the acceleration zone increase clearly compared with the original percentage (before electrophoresis), indicating the concentration effect because of center contraction of the circle. The above results show the potential to separate nanoparticles with high precision under the circular non-uniform electric field in horizontal.

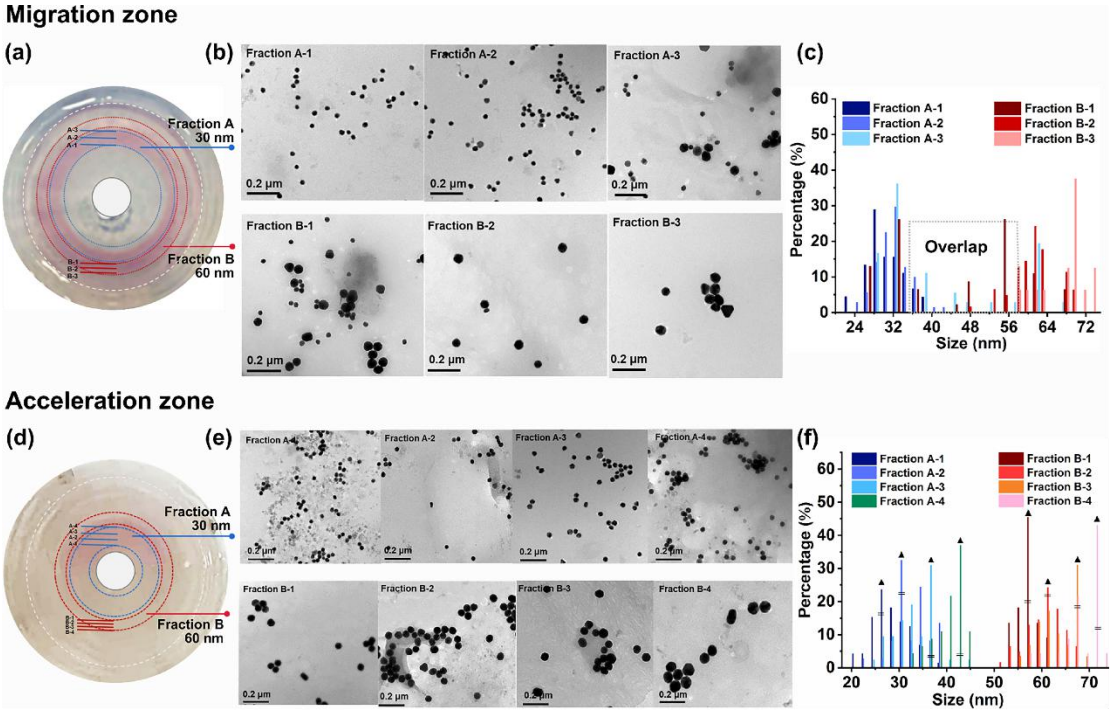

Figure 5. Electrophoresis separation and analysis of 30 nm and 60 nm AuNPs in migration zone and acceleration zone under the circular non-uniform electric field in horizontal. The experiment was performed under the 0.8% agarose gel, voltage was 75 V and the buffer solution was 1×TBE (pH=8.2). (a, d) images of electrophoresis separation, (b, e) typical TEM images of AuNPs from different fractions of the corresponding electrophoresis bands, (c, f) size distributions of AuNPs from different fractions, calculated by TEM data. The total numbers of nanoparticles were analyzed by using the software ImageJ. Each sample showed more than 100 particles to provide a good representativeness of the separation results. In Figure f, ▲ represents the percentage of AuNPs after electrophoresis and ═ represents the percentage before electrophoresis.

In all of the above experiments, two electrodes of equal length generate the non-uniform electric field with equivalent electric intensity and parallel equipotential lines in longitudinal. As a result, the nanoparticles pass through the migration zone, acceleration zone, and concentration

zone for highly precise separation along the equipotential lines without longitudinal focusing. In view of this, the trend of equipotential lines is controlled for simultaneous separation and concentration. As shown in Figure 6a, two parallel electrodes with difference in height produce the non-uniform electric field in both horizontal and vertical, presenting parabolic electric field lines (defined as non-uniform field 2). In horizontal, the electric intensity also gradually decreases along with the radius from center to edge with the concentric equipotential lines (Figure 6b, c), and the integration is shown in Figure 6d. In longitudinal, the electric intensity is unequal located at the top, middle, and bottom (Figure 6e). Therefore, the same nanoparticles are subject to the different forces in longitudinal under the same q and f′, except for the gradient force in horizontal. The nanoparticles would be driven by the stronger electrophoretic force (F_{ep}) point to the positive electrode along the oblique electric field lines, contributing to concentration in both horizontal and longitudinal (Figure 6f). The circular non-uniform field would prompt the simultaneous target-type separation and concentration of different target nanoparticles, which would ultimately be collected one by one in the center of a circle (Figure 6g).

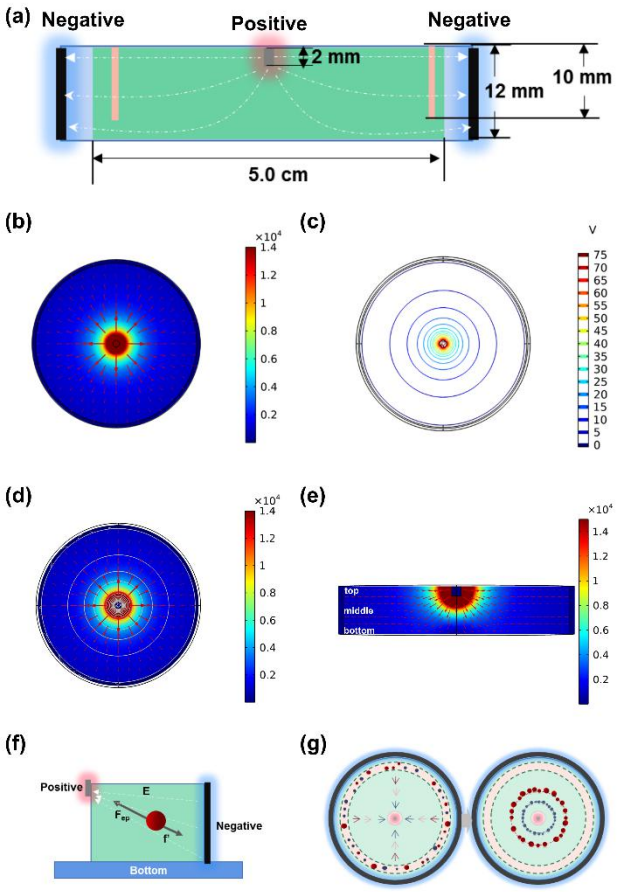

Figure 6 . (a) Scheme of relative position of negative and positive electrodes. COMSOL simulation of circular non-uniform field 2. (b) electric intensity, (c) equipotential lines, (d) integration of electric intensity and equipotential line, (e) cross section, (f) Force analysis of nanoparticle in circular non-uniform field 2 (the voltage was set at 75 V). F_{ep} represents electrophoretic force and f′ represents viscous force. (g) Scheme of target-type concentration of nanoparticles with different sizes under circular non-uniform field 2.

In addition to this, the curve of electric field intensity and radius from COMSOL simulation explicitly reveals the variation of electric field intensity in horizontal and longitudinal under the circular non-uniform electric field 2 (Figure 7). The electric field intensity is very small closer to zero at the bottom, and it increases exponentially with the reduction of radius at the top and

middle. The electric field intensity at the top is bigger than that at the middle in the migration zone and acceleration zone, so the relatively uniform electric field could drive nanoparticles lateral movement for separation (radius > 1.5 cm). Nevertheless, when the radius less than 0.6 cm belongs to the concentration zone, the electric field intensity at the middle is over at the top, promoting the longitudinal migration of nanoparticles towards the central electrode along the electric field lines. The nanoparticles tend to be gradually extruded in the concentration zone, that is, sample concentration. That is to say, the circular non-uniform electric field can control the trend of electric field line in migration zone, acceleration zone, and concentration zone to achieve the target-type, controlled, precise separation, and concentration.

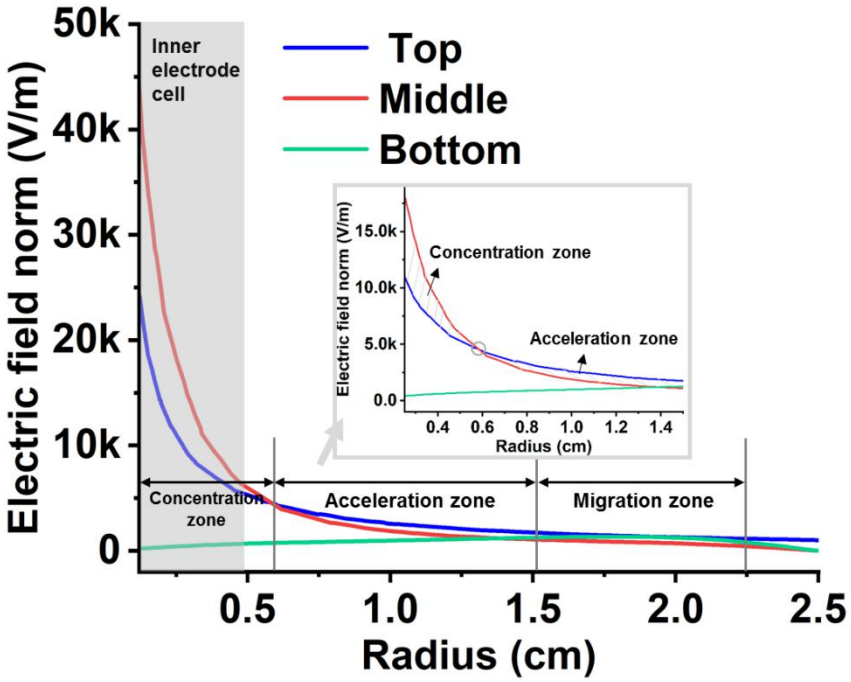

Figure 7. Typical curve of electric field norm and radius from simulation for the circular non-uniform electric field 2 in horizontal and longitudinal (The voltage was set at 75 V).

As expected, the bands of 30 and 60 nm AuNPs are long, thin, and highlighted without band

dispersion in space due to the additional non-uniform electric field in longitudinal with extrusion effect for concentration (Figure 8). The discrepancies of migration velocities bring about separation of 30 and 60 nm AuNPs with two concentric circle bands in migration zone, the separation resolution and extrusion effect improve gradually in acceleration zone, which is consistent with the results of field simulation. Similar results are also obtained by comparing migration behaviors of nanoparticles under non-uniform fields 1 and 2 (Figure S4). Therefore, it's available for simultaneous separation and concentration of nanoparticles via controlling electric field line type in different function zones of the circular non-uniform electric field.

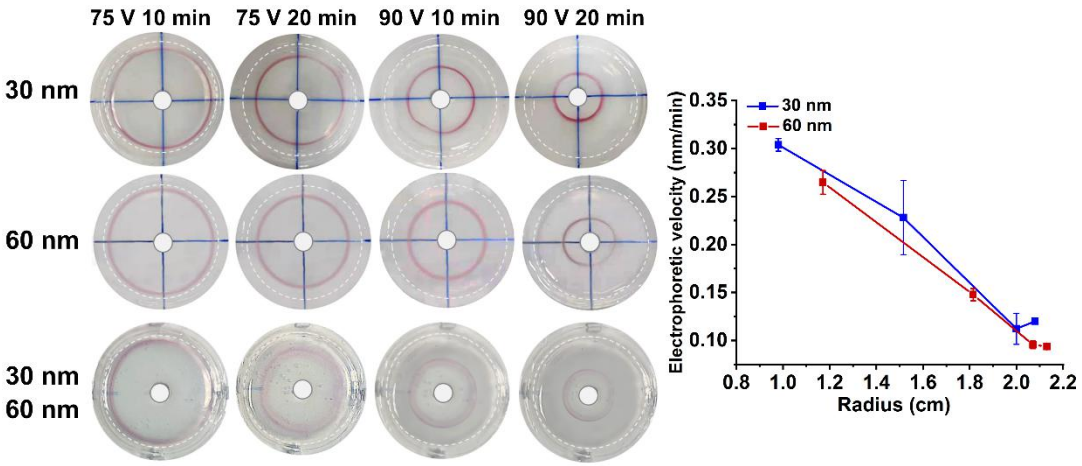

Figure 8. Electrophoresis migration and electrophoretic velocity analysis of 30 and 60 nm AuNPs under the circular non-uniform electric field 2. The experiment was performed under the 0.8 % agarose gel, the buffer solution was 1×TBE (pH=8.2).

The slab gel electrophoresis is a classical method to separate the biomacromolecule under uniform electric field, which has been attempted to sort nanoparticles, DNA, exosomes. Compared with the circular non-uniform electric field, the bands of AuNPs are dispersive without the clear boundary for separation without any concentration effect after the slab gel electrophoresis (Figure

S5). The slab-type uniform electric field shape generates the same electric field intensity with parallel electric field lines between positive and negative electrodes, resulting in one-dimensional migration of particles without any directional focusing. By contrast, the circular non-uniform electric field can provide synchronous dual actions of extrusion in longitudinal and concentric converging in horizontal, accompanied by separation effect of gradient electric field intensity. The concentration effect is distinct under the non-uniform electric field strategy, especially non-uniform electric field 2. Under non-uniform field 1, the concentration multiple is 1.7 times calculated by radius ratio, and even up to 19.8 times under non-uniform field 2 calculated by volume ratio (Figure S6). Through the further simple improvement of the equipment, the loading sample amount can be increased arbitrarily to improve the concentration multiple. Therefore, the concentric non-uniform field gel electrophoresis has the ability to achieve both separation and concentration of particles.

Conclusion

In this work, the target-type non-uniform field gel electrophoresis has been proposed for precise separation and efficient concentration by controlling types of electric field lines. Under the circular non-uniform electric field, the electric field intensity increases exponentially from outer edge to center with different functional zones of migration, acceleration, and concentration. The 30 and 60 nm AuNPs are separated precisely with an average size difference of about 5 nm by controlling the parallel-type electric field line in longitudinal. Furthermore, the migration of 30 and 60 nm AuNPs is controlled for simultaneous concentric-type separation and concentration by regulating parabolic electric field lines in longitudinal of the acceleration and concentration zone.

The concept of a target-type non-uniform field system has a great potential to attain separation and preparation of various biomacromolecules (e.g. DNA, RNA, exosomes, virus) for accurate therapy; and also apply in microplastics analysis in environment, high-throughput nano-bioreactor and assembly.

Supporting Information

Figure S1. Device fabrication. **Figure S2.** The heating effect, temperature and pH value under the circular non-uniform electric field. **Figure S3.** Analysis of 30 and 60 nm AuNPs electrophoresis bands obtained under the circular non-uniform electric field in horizontal. **Figure S4.** Electrophoresis migration and electrophoretic velocity analysis of 30 and 60 nm AuNPs under the circular non-uniform electric field 1 and 2. **Figure S5.** Electrophoresis migration and typical TEM images of 30 and 60 nm AuNPs after the slab gel electrophoresis. **Figure S6.** Calculation of concentration effect under the non-uniform electric field strategy.

Conflicts of interest

The authors declare no competing financial interest.

Acknowledgements

This study was supported by grants from the National Natural Science Foundation of China (No. 22176164, 21775134, 21904113) and Overseas Expertise Introduction Project for Discipline Innovation of China (111 Project, No. D18012), China.

References

(1) Zhang, H.; Lyden, D. Asymmetric-Flow Field-Flow Fractionation Technology for Exomere and Small Extracellular Vesicle Separation and Characterization. *Nat. Protoc.* **2019**, 14, 1027-1053.

(2) Gu, Y.; Chen, C.; Mao, Z.; Bachman, H.; Becker, R.; Rufo, J.; Wang, Z.; Zhang, P.; Mai, J.; Yang, S.; Zhang, J.; Zhao, S.; Ouyang, Y.; Wong, D. T. W.; Sadovsky, Y.; Huang, T. J. Acoustofluidic Centrifuge for Nanoparticle Enrichment and Separation. *Sci.Adv.* **2021**, 7, eabc0467.

(3) Zhang, K.; Ren, Y.; Tao, Y.; Liu, W.; Jiang, T.; Jiang, H. Efficient Micro/Nanoparticle Concentration Using Direct Current-Induced Thermal Buoyancy Convection for Multiple Liquid Media. *Anal. Chem.* **2019**, 91, 4457-4465.

(4) Liu, C.; Guo, J.; Tian, F.; Yang, N.; Yan, F.; Ding, Y.; Wei, J.; Hu, G.; Nie, G.; Sun, J. Field-Free Isolation of Exosomes from Extracellular Vesicles by Microfluidic Viscoelastic Flows. *ACS Nano* **2017**, 11, 6968-6976.

(5) Trung, N. T.; Hien, T. T.; Huyen, T. T.; Quyen, D. T.; Van Son, T.; Hoan, P. Q.; Phuong, N. T.; Lien, T. T.; Binh, M. T.; Van Tong, H.; Meyer, C. G.; Velavan, T. P.; Song le, H. Enrichment of Bacterial DNA for the Diagnosis of Blood Stream Infections. *BMC Infect Dis* **2016**, 16, 235.

(6) Marczak, S.; Richards, K.; Ramshani, Z.; Smith, E.; Senapati, S.; Hill, R.; Go, D. B.; Chang, H. C. Simultaneous Isolation and Preconcentration of Exosomes by Ion Concentration Polarization. *Electrophoresis* **2018**, 39, 2029-2038.

(7) Yang, H. C.; Ham, Y. M.; Kim, J. A.; Rhee, W. J. Single-Step Equipment-Free Extracellular Vesicle Concentration Using Super Absorbent Polymer Beads. *J. Extracell Vesicles* **2021**, 10, e12074.

(8) Chen, Y.; Zhu, Q.; Cheng, L.; Wang, Y.; Li, M.; Yang, Q.; Hu, L.; Lou, D.; Li, J.; Dong, X.; Lee, L. P.; Liu, F. Exosome Detection Via the Ultrafast-Isolation System: Exodus. *Nat. Methods* **2021**, 18, 212-218.

(9) Liu, S.; Yuzvinsky, T. D.; Schmidt, H. Effect of Fabrication-Dependent Shape and Composition of Solid-State Nanopores on Single Nanoparticle Detection. *ACS Nano* **2013**, 7, 5621-5627.

(10) Hassanpour Tamrin, S.; Sanati Nezhad, A.; Sen, A. Label-Free Isolation of Exosomes Using Microfluidic Technologies. *ACS Nano* **2021**, 15, 17047-17079.

(11) Lozano-Ramos, I.; Bancu, I.; Oliveira-Tercero, A.; Armengol, M. P.; Menezes-Neto, A.; Del Portillo, H. A.; Lauzurica-Valdemoros, R.; Borras, F. E. Size-Exclusion Chromatography-Based Enrichment of Extracellular Vesicles from Urine Samples. *J Extracell Vesicles* **2015**, 4, 27369.

(12) Latham, A. H.; Freitas, R. S.; Schiffer, P.; Williams, M. E. Capillary Magnetic Field Flow Fractionation and Analysis of Magnetic Nanoparticles. *Anal. Chem.* **2005**, 77, 5055-5062.

(13) Shendruk, T. N.; Tahvildari, R.; Catafard, N. M.; Andrzejewski, L.; Gigault, C.; Todd, A.; Gagne-Dumais, L.; Slater, G. W.; Godin, M. Field-Flow Fractionation and Hydrodynamic Chromatography on a Microfluidic Chip. *Anal. Chem.* **2013**, 85, 5981-5988.

(14) Lu, X.; Xuan, X. Elasto-Inertial Pinched Flow Fractionation for Continuous Shape-Based Particle Separation. *Anal. Chem.* **2015**, 87, 11523-11530.

(15) Yamada, M.; Nakashima, M.; Seki, M. Pinched Flow Fractionation: Continuous Size Separation of Particles Utilizing a Laminar Flow Profile in a Pinched Microchannel. *Anal. Chem.* **2004**, 76, 5465-5471.

(16) De Paoli, P.; Villalta, D.; Battistin, S.; Gasparollo, A.; Santini, G. Selective Loss of Okt8 Lymphocytes on Density Gradient Centrifugation Separation of Blood Mononuclear Cells. *J Immunol Methods* **1983**, 61, 259-260.

(17) Wang, B.; Weldon, A. L.; Kumnorkaew, P.; Xu, B.; Gilchrist, J. F.; Cheng, X. Effect of Surface Nanotopography on Immunoaffinity Cell Capture in Microfluidic Devices. *Langmuir* **2011**, 27, 11229-11237.

(18) Woo, H. K.; Sunkara, V.; Park, J.; Kim, T. H.; Han, J. R.; Kim, C. J.; Choi, H. I.; Kim, Y. K.; Cho, Y. K. Exodisc for Rapid, Size-Selective, and Efficient Isolation and Analysis of Nanoscale Extracellular Vesicles from Biological Samples. *ACS Nano* **2017**, 11, 1360-1370.

(19) Liu, F.; Vermesh, O.; Mani, V.; Ge, T. J.; Madsen, S. J.; Sabour, A.; Hsu, E. C.; Gowrishankar, G.; Kanada, M.; Jokerst, J. V.; Sierra, R. G.; Chang, E.; Lau, K.; Sridhar, K.; Bermudez, A.; Pitteri, S. J.; Stoyanova, T.; Sinclair, R.; Nair, V. S.; Gambhir, S. S.; Demirci, U. The Exosome Total Isolation Chip. *ACS Nano* **2017**, 11, 10712-10723.

(20) Wang, Z.; Wu, H. J.; Fine, D.; Schmulen, J.; Hu, Y.; Godin, B.; Zhang, J. X.; Liu, X. Ciliated Micropillars for the Microfluidic-Based Isolation of Nanoscale Lipid Vesicles. *Lab Chip* **2013**, 13, 2879-2882.

(21) DNA Manipulation and Separation in Sublithographic-Scale Nanowire Array. *ACS Nano* **2013**, 7, 3029-3035.

(22) Yasui, T.; Yanagida, T.; Ito, S.; Konaka De , Y.; Takeshita, D. Unveiling Massive Numbers of Cancer-Related Urinary-Microrna Candidates via Nanowires. *Sci. Adv.* **2017**, 3, e1701133.

(23) Tottori, N.; Nisisako, T. Degas-Driven Deterministic Lateral Displacement in Poly(Dimethylsiloxane) Microfluidic Devices. *Anal. Chem.* **2019**, 91, 3093-3100.

(24) Hochstetter, A.; Vernekar, R.; Austin, R. H.; Becker, H.; Beech, J. P.; Fedosov, D. A.; Gompper, G.; Kim, S. C.; Smith, J. T.; Stolovitzky, G.; Tegenfeldt, J. O.; Wunsch, B. H.; Zeming, K. K.; Kruger, T.; Inglis, D. W. Deterministic Lateral Displacement: Challenges and Perspectives. *ACS Nano* **2020**, 14, 10784-10795.

(25) Kim, J. A.; Lee, J. R.; Je, T. J.; Jeon, E. C.; Lee, W. Size-Dependent Inertial Focusing Position Shift and Particle Separations in Triangular Microchannels. *Anal. Chem.* **2018**, 90, 1827-1835.

(26) Anja; Kunze; Peter; Tseng; Chanya; Godzich; Coleman; Murray; Anna; Caputo. Engineering Cortical Neuron Polarity with Nanomagnets on a Chip. *ACS Nano* **2015**, 9, 3664-3676.

(27) Lim, J. K.; Lanni, C.; Evarts, E. R.; Lanni, F.; Tilton, R. D.; Majetich, S. A. Magnetophoresis of Nanoparticles. *ACS Nano* **2011**, 5, 217-226.

(28) Bekdemir, A.; Stellacci, F. A Centrifugation-Based Physicochemical Characterization Method for the Interaction between Proteins and Nanoparticles. *Nat. Commun.* **2016**, 7, 13121.

(29) Arosio, P.; Muller, T.; Mahadevan, L.; Knowles, T. P. Density-Gradient-Free Microfluidic Centrifugation for Analytical and Preparative Separation of Nanoparticles. *Nano Lett.* **2014**, 14, 2365-2371.

(30) Al-Faqheri, W.; Thio, T. H. G.; Qasaimeh, M. A.; Dietzel, A.; Madou, M.; Al-Halhouli, A. a. Particle/Cell Separation on Microfluidic Platforms Based on Centrifugation Effect: A Review. *Microflui. Nanofluid.* **2017**, 21, 102.

(31) Davies, R. T.; Kim, J.; Jang, S. C.; Choi, E. J.; Gho, Y. S.; Park, J. Microfluidic Filtration System to Isolate Extracellular Vesicles from Blood. *Lab Chip* **2012**, 12, 5202-5210.

(32) Liu, P.; Tian, Z.; Hao, N.; Bachman, H.; Zhang, P.; Hu, J.; Huang, T. J. Acoustofluidic Multi-Well Plates for Enrichment of Micro/Nano Particles and Cells. *Lab Chip* **2020**, 20, 3399-3409.

(33) Gai, J.; Nosrati, R.; Neild, A. High DNA Integrity Sperm Selection Using Surface Acoustic Waves. *Lab Chip* **2020**, 20, 4262-4272.

Soikkeli, M.; Seppa, T.; Tuunainen, E.; Spangar, A.; von Lode, P.; Rantakokko-Jalava, K.; Otto, G.; Scheding, S.; Soukka, T.; Wittfooth, S.; Laurell, T. Integrated Acoustic Separation, Enrichment, and Microchip Polymerase Chain Reaction Detection of Bacteria from Blood for Rapid Sepsis Diagnostics. *Anal. Chem.* **2016**, 88, 9403-9411.

(35) Gustafson, K. T.; Huynh, K. T.; Heineck, D.; Bueno, J.; Modestino, A.; Kim, S.; Gower, A.; Armstrong, R.; Schutt, C. E.; Ibsen, S. D. Automated Fluorescence Quantification of Extracellular Vesicles Collected from Blood Plasma Using Dielectrophoresis. *Lab Chip* **2021**, 21, 1318-1332.

(36) Park, S.; Zhang, Y.; Wang, T. H.; Yang, S. Continuous Dielectrophoretic Bacterial Separation and Concentration from Physiological Media of High Conductivity. *Lab Chip* **2011**, 11, 2893-2900.

(37) Xu, J.; Kwak, K. J.; Lee, J. L.; Agarwal, G. Lifting and Sorting of Charged Au Nanoparticles by Electrostatic Forces in Atomic Force Microscopy. *Small* **2010**, 6, 2105-2108.

(38) Ho, C. T.; Lin, R. Z.; Chang, W. Y.; Chang, H. Y.; Liu, C. H. Rapid Heterogeneous Liver-Cell on-Chip Patterning via the Enhanced Field-Induced Dielectrophoresis Trap. *Lab Chip* **2006**, 6, 724-734.

(39) Ibsen, S. D.; Wright, J.; Lewis, J. M.; Kim, S.; Ko, S. Y.; Ong, J.; Manouchehri, S.; Vyas, A.; Akers, J.; Chen, C. C.; Carter, B. S.; Esener, S. C.; Heller, M. J. Rapid Isolation and Detection of Exosomes and Associated Biomarkers from Plasma. *ACS Nano* **2017**, 11, 6641-6651.

(40) Hanauer, M.; Pierrat, S.; Zins, I.; Lotz, A.; Sonnichsen, C. Separation of Nanoparticles by Gel Electrophoresis According to Size and Shape. *Nano Lett.* **2007**, 7, 2881-2885.

(41) Zhang, Y.; Deng, Z.; Lou, D.; Wang, Y.; Wang, R.; Hu, R.; Zhang, X.; Zhu, Q.; Chen, Y.; Liu, F. High-Efficiency Separation of Extracellular Vesicles from Lipoproteins in Plasma by Agarose Gel Electrophoresis. *Anal. Chem.* **2020**, 92, 7493-7499.

(42) Li, F.; Hill, R. J. Nanoparticle Gel Electrophoresis: Bare Charged Spheres in Polyelectrolyte Hydrogels. *J Colloid Interf. Sci.* **2013**, 394, 1-12.

(43) Zheng, Y.; Hong, Y.; Wu, W.; Sun, D.; Wang, Y.; Huang, J.; Li, Q. Separation of Different Shape Biosynthesized Gold Nanoparticles via Agarose Gel Electrophoresis. *Sep. Purif. Technol.* **2015**, 151, 332-337.

For Table of Contents Only

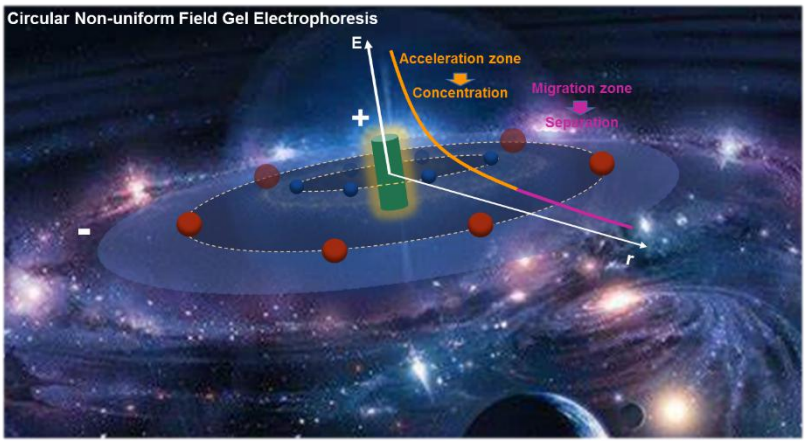

A target-type non-uniform field gel electrophoresis methodology was developed to control the migration behaviors of nanoparticles for precise separation and concentration.

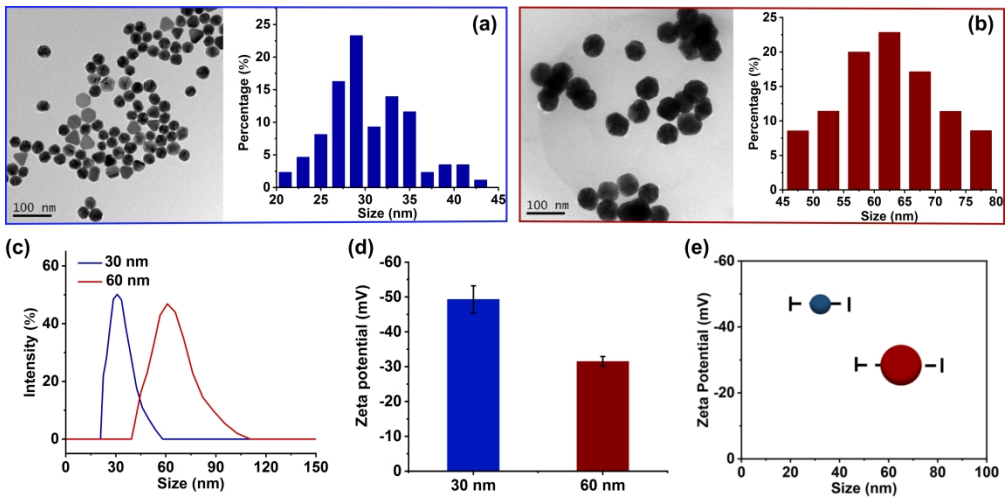

Figure 1. Typical TEM images of AuNPs and size distribution calculated by corresponding TEM data: (a) 30 nm, (b) 60 nm, the total numbers of nanoparticles were analyzed by using the software ImageJ. Each sample showed more than 100 particles to provide a good representativeness of the separation results. (c) Size distribution measured by DLS, (d) Zeta potential of AuNPs, (d) Comparison of size and zeta potential of 30 nm (blue) and 60 nm (red) AuNPs.

517x253mm (236 x 236 DPI)

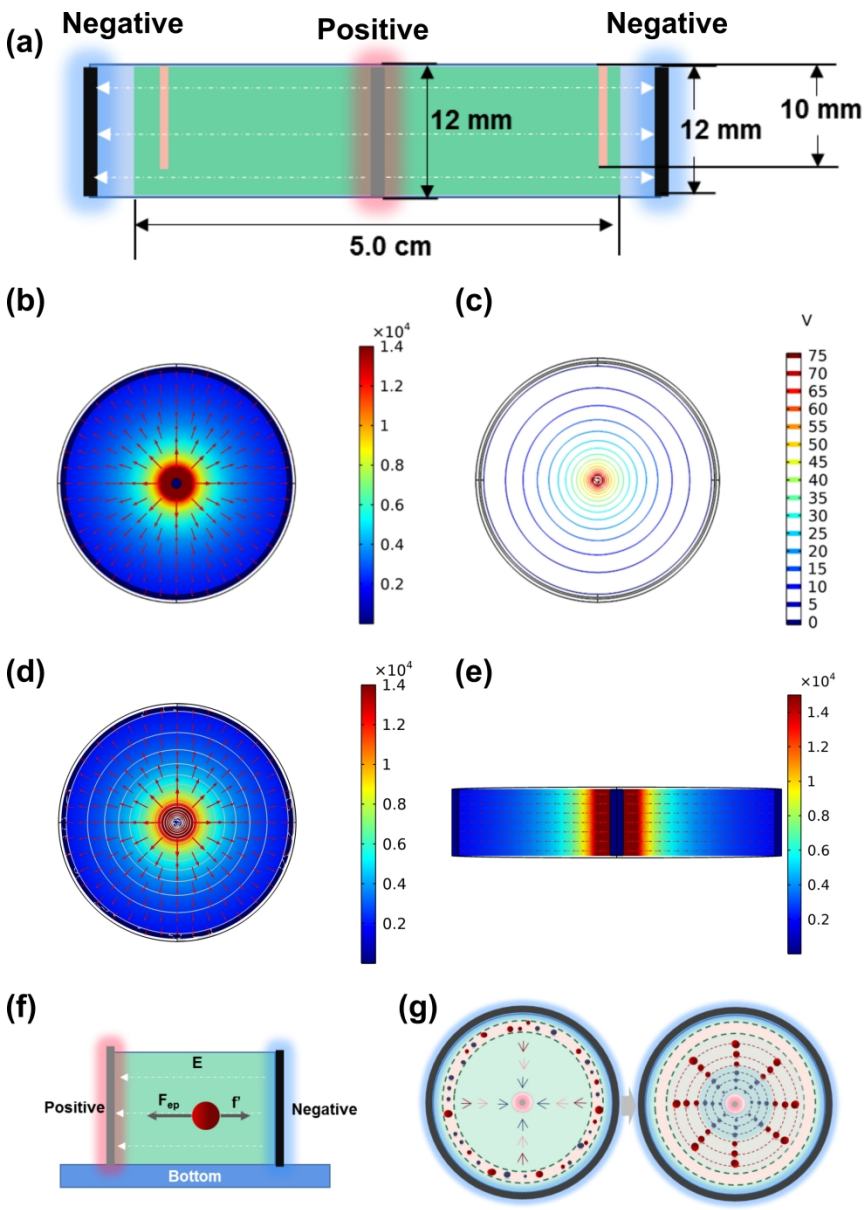

Figure 2. (a) Scheme of relative position of negative and positive electrodes. COMSOL simulation of circular non-uniform field 1. (b) electric field intensity, (c) equipotential lines, (d) integration of electric intensity and equipotential line, (e) cross section, (f) Force analysis of nanoparticle under circular non-uniform field 1 (the voltage was set at 75 V). Fep represents the electrophoretic force and f′ represents the viscous force. (g) Scheme of precise target-type distribution of nanoparticles with size difference under circular non-uniform field 1.

349x476mm (236 x 236 DPI)

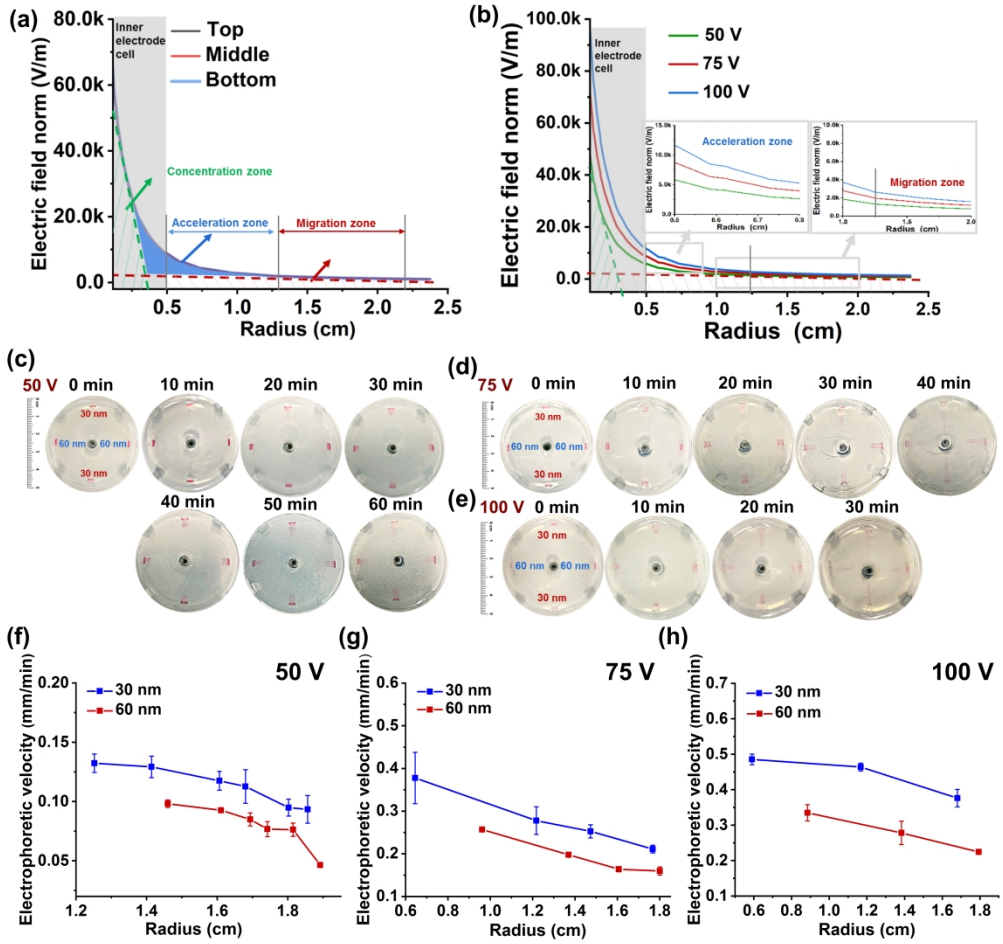

Figure 4. (a) Typical curve of electric field norm and radius from COMSOL simulation for the circular non-uniform electric field 1 in horizontal and longitudinal (75 V). (b) Comparison of curves of electric field norm and radius at different voltages from COMSOL simulation (50 V, 75 V, 100 V). (c-e) Migration images of 30 nm and 60 nm AuNPs with electrophoresis time at different voltages. (f-h) Comparison of the electrophoretic velocity of 30 nm and 60 nm AuNPs at 50, 75 and 100 V voltage, respectively. The experiment was performed under the 0.8% agarose gel and the 1×TBE (pH=8.2) buffer solution.

523x493mm (236 x 236 DPI)

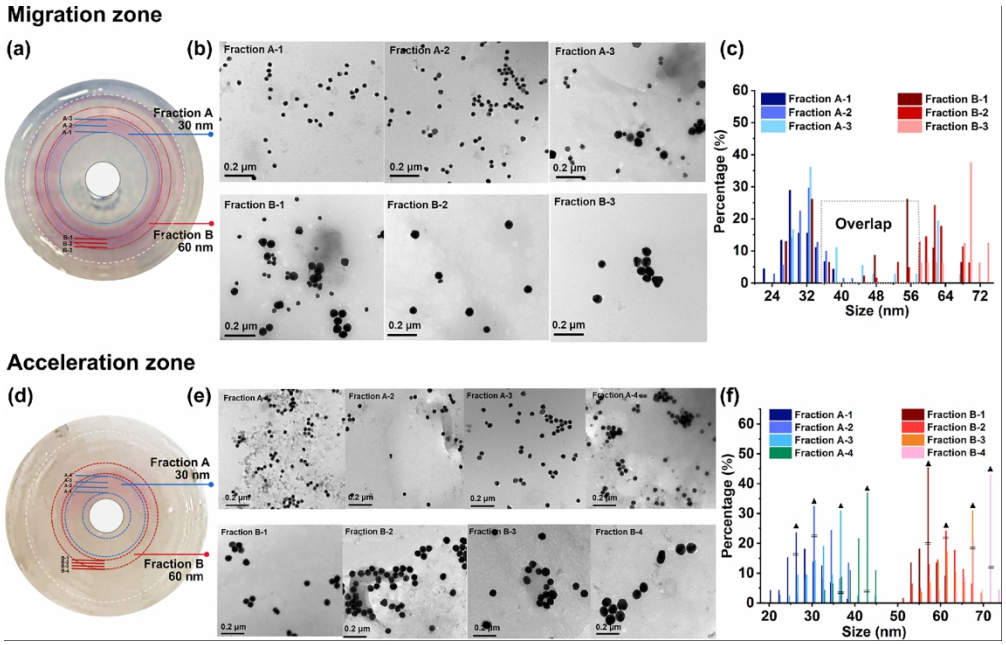

Figure 5. Electrophoresis separation and analysis of 30 nm and 60 nm AuNPs in migration zone and acceleration zone under the circular non-uniform electric field in horizontal. The experiment was performed under the 0.8% agarose gel, voltage was 75 V and the buffer solution was 1×TBE (pH=8.2). (a, d) images of electrophoresis separation, (b, e) typical TEM images of AuNPs from different fractions of the corresponding electrophoresis bands, (c, f) size distributions of AuNPs from different fractions, calculated by TEM data. The total numbers of nanoparticles were analyzed by using the software ImageJ. Each sample showed more than 100 particles to provide a good representativeness of the separation results. In Figure f, ▲ represents the percentage of AuNPs after electrophoresis and ═ represents the percentage before electrophoresis.

291x185mm (300 x 300 DPI)

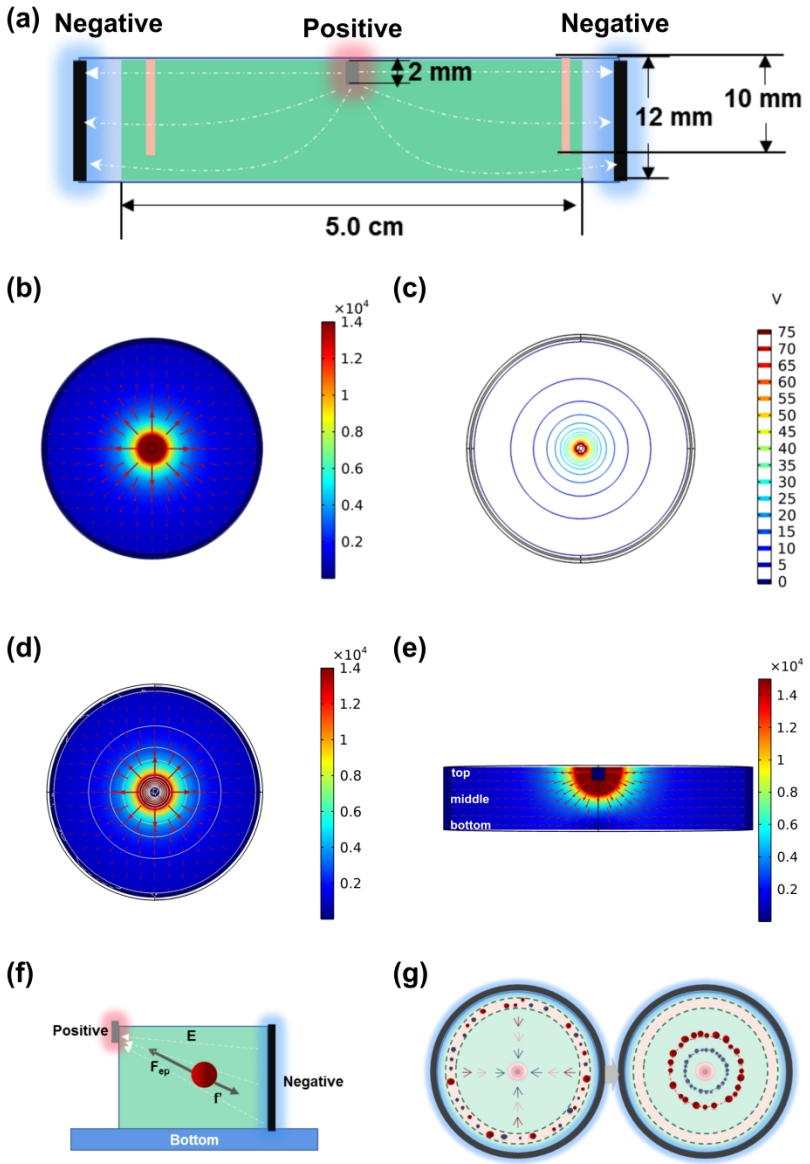

Figure 6. (a) Scheme of relative position of negative and positive electrodes. COMSOL simulation of circular non-uniform field 2. (b) electric intensity, (c) equipotential lines, (d) integration of electric intensity and equipotential line, (e) cross section, (f) Force analysis of nanoparticle in circular non-uniform field 2 (the voltage was set at 75 V). Fep represents electrophoretic force and f′ represents viscous force. (g) Scheme of target-type concentration of nanoparticles with different sizes under circular non-uniform field 2.

385x535mm (236 x 236 DPI)

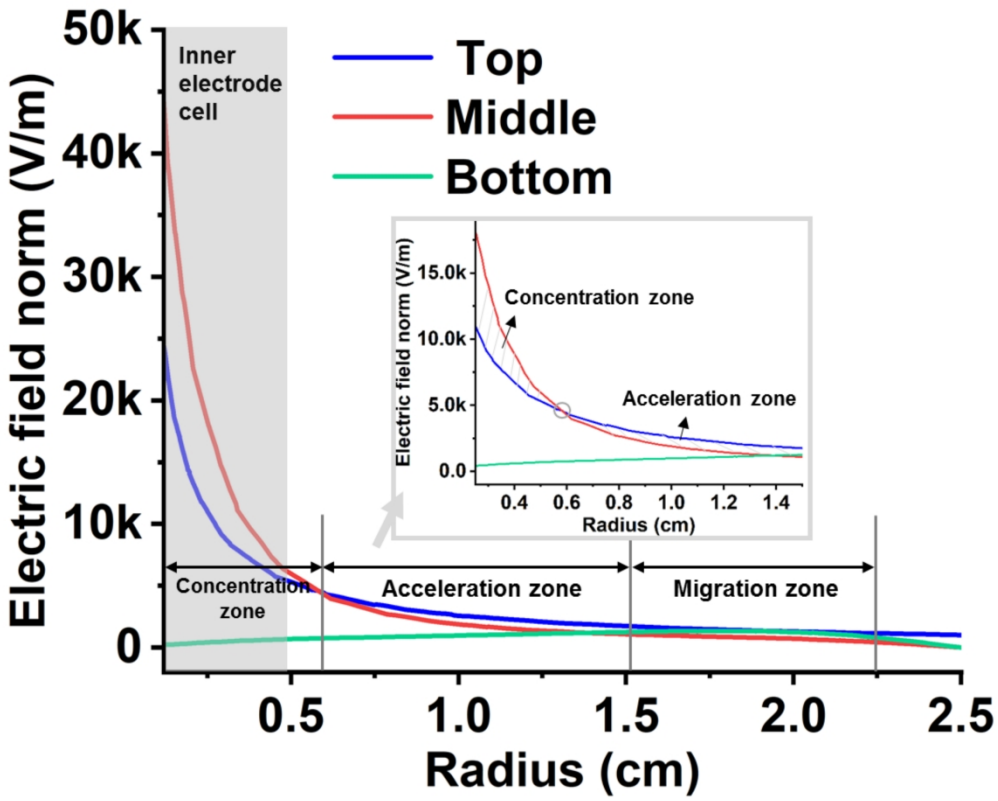

Figure 7. Typical curve of electric field norm and radius from simulation for the circular non-uniform electric field 2 in horizontal and longitudinal (The voltage was set at 75 V).

398x318mm (236 x 236 DPI)

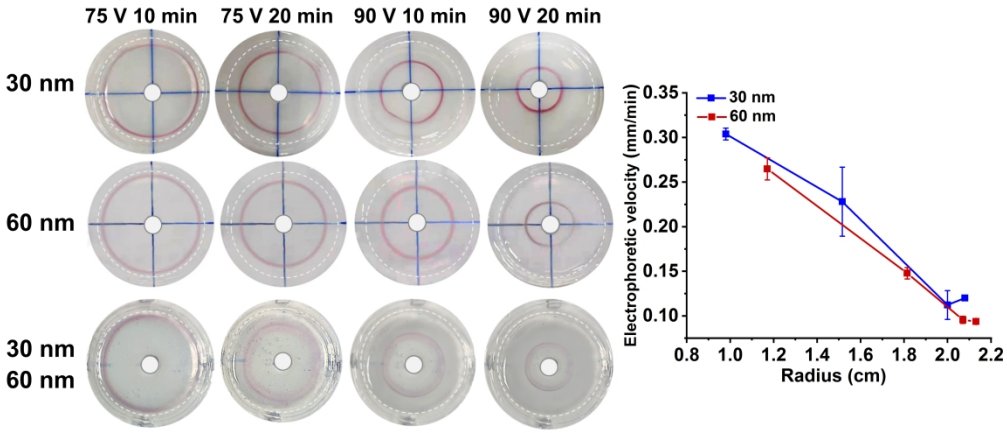

Figure 8. Electrophoresis migration and electrophoretic velocity analysis of 30 and 60 nm AuNPs under the circular non-uniform electric field 2. The experiment was performed under the 0.8% agarose gel, the buffer solution was 1×TBE (pH=8.2).

525x235mm (236 x 236 DPI)

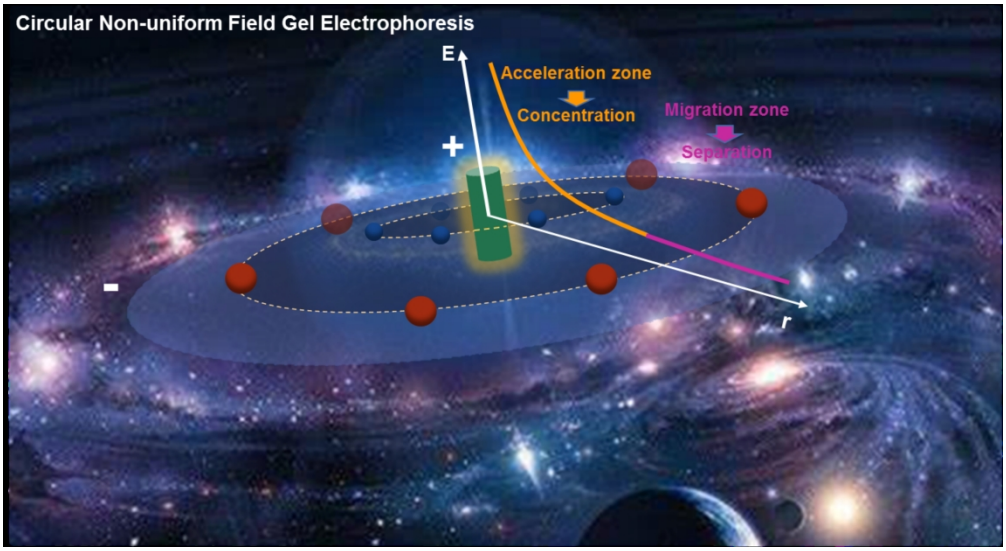

TOC

530x287mm (236 x 236 DPI)